

IMPEDANCE-BASED FAULT LOCATION EXPERIENCE

Karl Zimmerman and David Costello
Schweitzer Engineering Laboratories, Inc.
Pullman, WA USA

INTRODUCTION

Accurate fault location reduces operating costs by avoiding lengthy and expensive patrols. Accurate fault location expedites repairs and restoration of lines, ultimately reducing revenue loss caused by outages.

In this paper, we describe one- and two-ended impedance-based fault location experiences. We define terms associated with fault location, and describe several impedance-based methods of fault location (simple reactance, Takagi, zero-sequence current with angle correction, and two-ended negative-sequence). We examine several system faults and analyze the performance of the fault locators given possible sources of error (short fault window, nonhomogeneous system, incorrect fault type selection, etc.).

Finally, we show the laboratory testing results of a two-ended method, where we automatically extracted a two-ended fault location estimate from a single end.

FAULT LOCATION METHODS AND DEFINITIONS

Several methods of estimating fault location are presently used in the field:

- DFR and short circuit data match
- Traveling wave methods
- Impedance-based methods
 - One-ended methods without using source impedance data (simple reactance, Takagi)
 - One-ended methods using source impedance data
- Two-ended methods

In this paper, we focus on certain impedance-based fault location methods and provide results from actual system faults.

NOTABLE IEEE DEFINITIONS

IEEE PC37.114, “Draft Guide for Determining Fault Location on AC Transmission and Distribution Lines”[1] was recently balloted and is in the approval process. One of the important contributions of the guide is the definitions section. Here are a few notable definitions found in the guide:

Fault location error: Percentage error in fault location estimate based on the total line length:
$$e(\text{error}) = (\text{instrument reading} - \text{exact distance to the fault}) / \text{total line length}.$$

For example, suppose a line is 100 miles long and the actual fault is 90 miles from the local terminal. If the local fault locator provides a fault location of 94 miles, the fault location error is

$(94-90)/100 = 4\%$. If the remote fault locator indicates 8 miles, the fault location error is $(8-10)/100 = 2\%$.

Homogeneous line: A transmission line where impedance is distributed uniformly on the whole length.

Examples of this are lines that use the same conductor size and construction throughout. Lines that are nonhomogeneous can be a source of error for one- or two-ended impedance-based fault location methods.

Homogeneous system: A transmission system where the local and remote source impedances have the same system angle as the line impedance. A homogeneous system is shown in Figure 1.

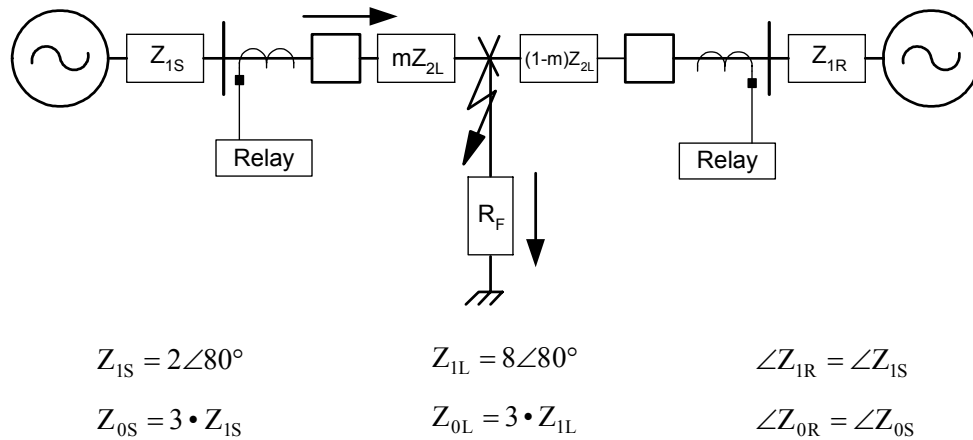


Figure 1 Example of a Homogeneous System

Nomograph: A graph that plots measured fault location versus actual fault location by compensating for known system errors.

Figure 2 shows a 69 kV line with 12.47 kV underbuild.

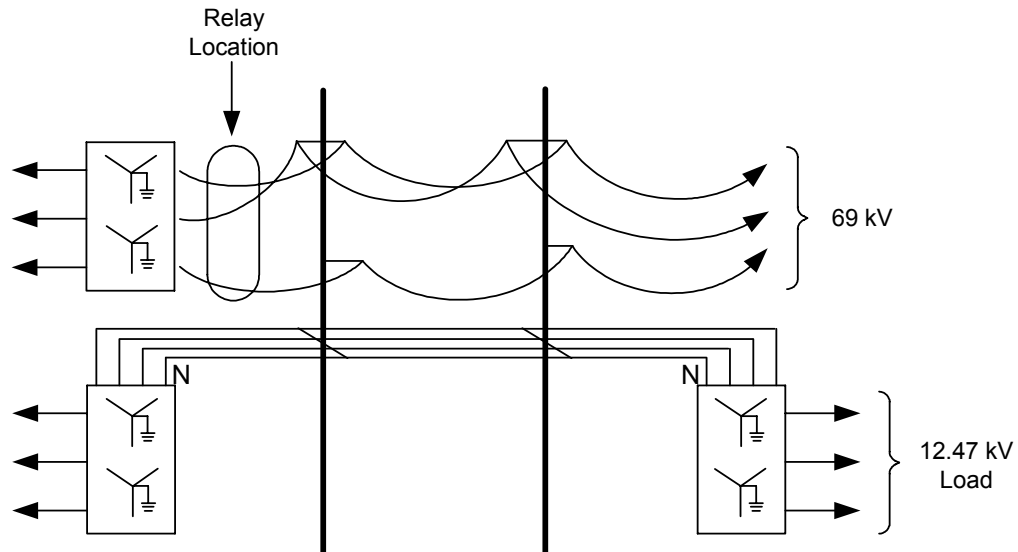


Figure 2 69 kV Line Configuration Sketch

How to build a nomograph:

1. Calculate line constants.
2. Determine which faults require a nomograph.
3. Using short circuit program, apply faults along the length of line (10%, 20%, etc.).
4. Plug resultant voltage and current values into fault location algorithms.
5. Plot a short circuit (actual) vs. calculated (relay) fault location.

	Without Underbuild	With 50 miles Underbuild
R1	7.50 Ω	7.50 Ω
X1	22.757 Ω	22.757 Ω
R0	21.327 Ω	15.488 Ω
X0	134.16 Ω	88.75 Ω

Figure 3 shows a completed nomograph.

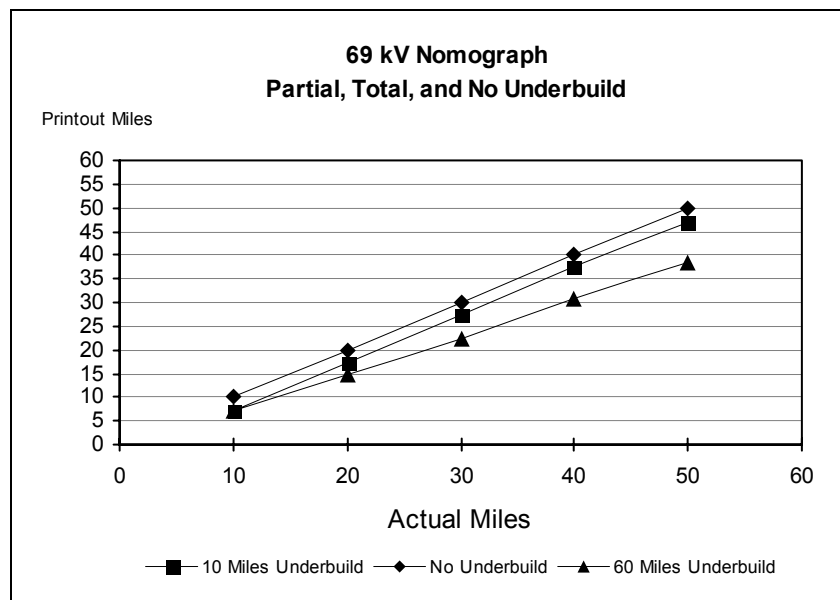


Figure 3 Completed Nomograph for 69 kV Line

IMPEDANCE-BASED FAULT LOCATION METHODS AND REQUIREMENTS

Impedance-based methods require the following approach:

1. Measure the voltage and current phasors.
2. Extract the fundamental components.
3. Determine the phasors and fault type.
4. Apply impedance algorithm.

One-ended impedance methods of fault location are a standard feature in most numerical relays. One-ended impedance methods use a simple algorithm, and communication channels and remote data are not required (except when a channel is required to bring the fault location estimate to an operator).

Two-ended methods can be more accurate but require data from both terminals. Data must be captured from both ends before an algorithm can be applied.

The most popular impedance-based fault location methods are discussed in this paper:

- Simple reactance method (one-ended)
- Takagi method (one-ended)
- Modified Takagi method that corrects for source impedance angle differences (one-ended)
- Two-ended negative-sequence method

One-ended impedance-based fault locators calculate the fault location from the apparent impedance seen by looking into the line from one end. An example system one-line is shown in Figure 4. To locate all fault types, the phase-to-ground voltages and currents in each phase must be measured. (If only line-to-line voltages are available, it is possible to locate phase-to-phase faults; if the zero-sequence source impedance, Z_0 , is known, we can estimate the location for phase-to-ground faults).

If the fault resistance is assumed to be zero, we can use one of the impedance calculations in Table 1 to estimate the fault location.

Table 1 Simple Impedance Equations

Fault Type	Positive-Sequence Impedance Equation ($mZ_{1L} =$)
A-ground	$V_a / (I_a + k \cdot 3 \cdot I_0)$
B-ground	$V_b / (I_b + k \cdot 3 \cdot I_0)$
C-ground	$V_c / (I_c + k \cdot 3 \cdot I_0)$
a-b or a-b-g	V_{ab} / I_{ab}
b-c or b-c-g	V_{bc} / I_{bc}
c-a or c-a-g	V_{ca} / I_{ca}
a-b-c	Any of the following: V_{ab} / I_{ab} , V_{bc} / I_{bc} , V_{ca} / I_{ca}

where

- k is $(Z_{0L} - Z_{1L}) / 3Z_{1L}$,
 Z_{0L} is the zero-sequence line impedance,
 Z_{1L} is the positive-sequence line impedance,
 m is the per unit distance to fault (for example: distance to fault in kilometers divided by the total line length in kilometers),
 I_0 is the zero-sequence current.

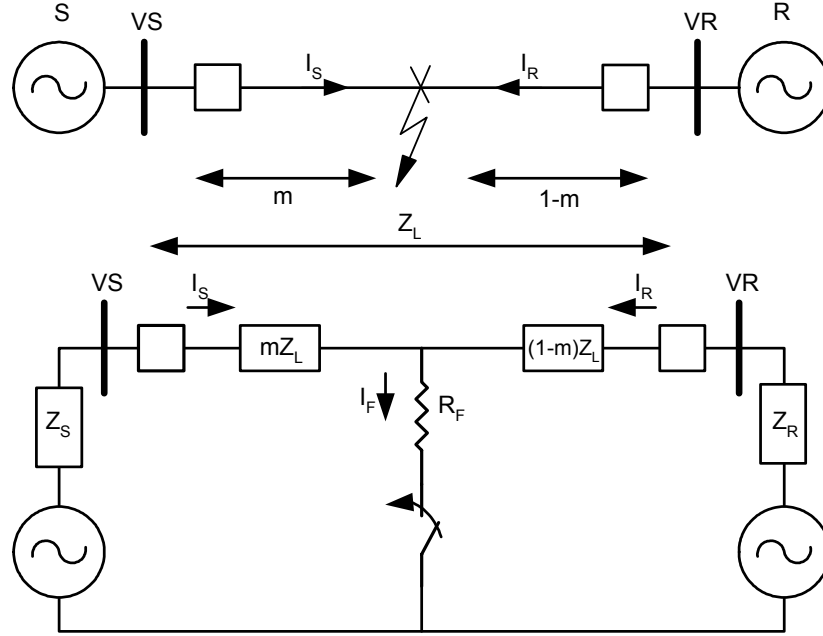


Figure 4 One-Line Diagram and Circuit Representation of Line Fault

The challenges for accuracy of one-ended fault location are well known and are described in several sources [1] [2] [3] [4]. To summarize, the following conditions can cause errors for one-ended impedance-based fault location methods:

- Combined effect of fault resistance and load
- Zero-sequence mutual coupling
- Zero-sequence modeling errors
- System nonhomogeneity
- System infeeds
 - Remote or third terminal infeed
 - Tapped load with zero-sequence source
- Inaccurate relay measurement, instrument transformer or line parameters.

Simple Reactance Method

From Figure 4, the voltage drop from the S end of the line is:

$$V_S = m \cdot Z_{IL} \cdot I_S + R_F \cdot I_F \quad (1)$$

For an A-phase to ground fault, $V_s = V_{a-g}$ and $I_S = I_a + k \cdot 3 \cdot I_0$.

The goal is to minimize the effect of the $R_F \cdot I_F$ term.

The simple reactance method divides all terms by I_S (I measured at the fault locator) and ignores the $(R_F \cdot I_F / I_S)$ term.

To do this, save the imaginary part, and solve for m :

$$\text{Im}(V_S/I_S) = \text{Im}(m \bullet Z_{IL}) = m \bullet X_{IL}$$

$$m = \frac{I_m \left(\frac{V_S}{I_S} \right)}{X_{IL}} \quad (2)$$

Error is 0 if $\angle I_S = \angle I_F$ or $R_F = 0$

Takagi Method—One-Ended Impedance Method With No Source Data

The Takagi method requires pre-fault and fault data. It improves upon the simple reactance method [2] by reducing the effect of load flow and minimizing the effect of fault resistance.

$$V_S = m \bullet Z_{IL} \bullet I + R_F \bullet I_F \quad (3)$$

Use Superposition current (I_{sup}) to find a term in phase with I_F :

$$I_{sup} = I - I_{pre}$$

$$I = \text{Fault Current} \quad (4)$$

$$I_{pre} = \text{Pre - fault Current}$$

Voltage drop from Bus S:

$$V_S = m \bullet Z_{IL} \bullet I_S + R_F \bullet I_F$$

Multiply both sides of equation (1) by the complex conjugate of I_{sup} (I_{sup}^*) and save the imaginary part. Then, solve for m :

$$\begin{aligned} I_m[V_S \bullet I_{sup}^*] &= m \bullet I_m(Z_{IL} \bullet I_S \bullet I_{sup}^*) + R_F \bullet I_m(I_F \bullet I_{sup}^*) \\ m &= \frac{I_m(V_S \bullet I_{sup}^*)}{I_m(Z_{IL} \bullet I_S \bullet I_{sup}^*)} \end{aligned} \quad (5)$$

The key to the success of the Takagi method is that the angle of I_S is the same as the angle of I_F . For an ideal homogeneous system, these angles are identical. As the angle between I_S and I_F increases, the error in the fault location estimate increases.

Modified Takagi—Zero-Sequence Current Method with Angle Correction

Another method (modified Takagi) uses zero-sequence current ($3 \bullet I_{0S}$) for ground faults instead of the superposition current. Therefore, this method requires no pre-fault data.

Modified Takagi also allows for angle correction. If the user knows the system source impedances, the zero-sequence current can be adjusted by angle T to improve the fault location estimate for a given line.

$$m = \frac{I_m (V_S \cdot (3 \cdot I_{0S})^* \cdot e^{-jT})}{I_m (Z_{1L} \cdot I_S \cdot (3 \cdot I_{0S})^* \cdot e^{-jT})} \quad (6)$$

The angle T selected will be valid for one fault location along the line. Figure 5 shows how to calculate T .

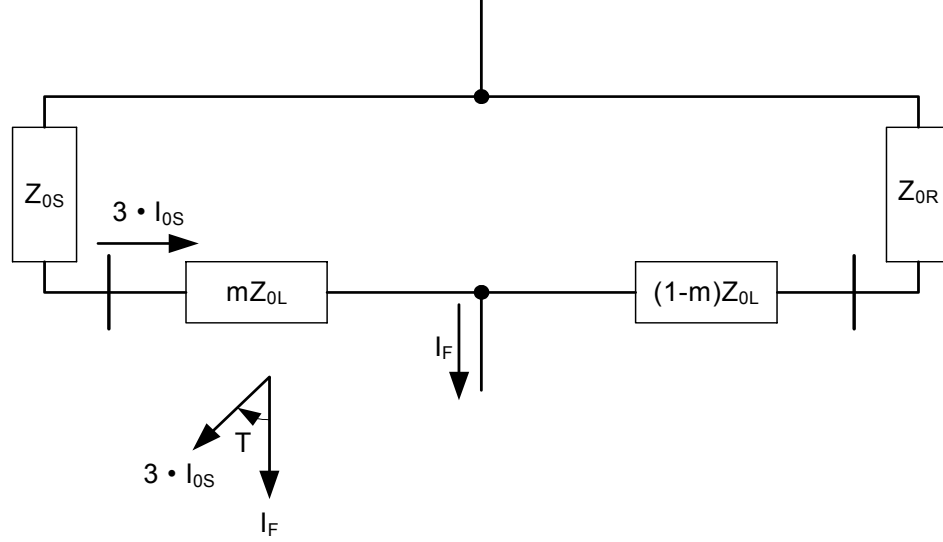


Figure 5 Zero-Sequence Current Angle Correction (if source impedances are known)

$$\frac{I_F}{3 \cdot I_{0S}} = \frac{Z_{0S} + Z_{0L} + Z_{0R}}{(1 - m) \cdot Z_{0L} + Z_{0R}} = A \angle T \quad (7)$$

Two-Ended Negative-Sequence Impedance Method

A relatively new method, introduced in 1999, uses negative-sequence quantities from all line terminals for the location of unbalanced faults. By using negative-sequence quantities, we negate the effect of prefault load and fault resistance, zero-sequence mutual impedance, and zero-sequence infeed from transmission line taps. Precise fault type selection is not necessary. Data alignment is not required because the algorithm employed at each line end uses the following quantities from the remote terminal (which do not require phase alignment).

- Magnitude of negative-sequence current, I_2
- Calculated negative-sequence source impedance, $Z_2 \angle \theta_2^\circ$

An observation from Figure 6 is that the negative-sequence fault voltage (V_{2F}) is the same when viewed from all ends of the protected line.

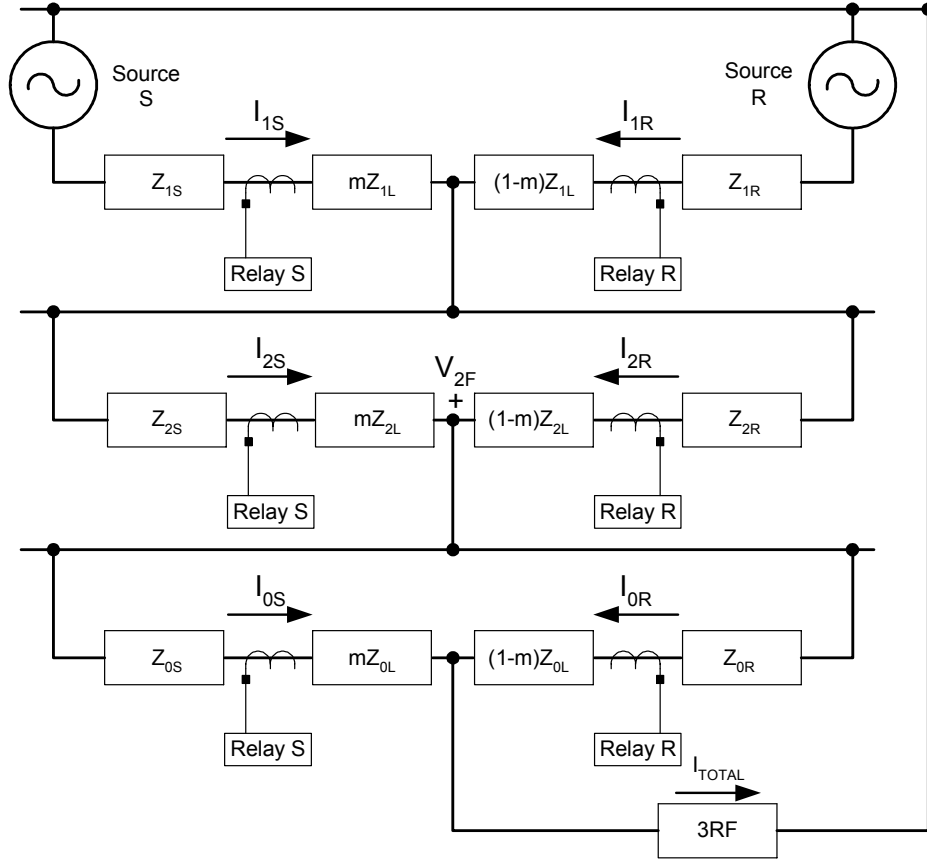


Figure 6 Connection of Sequence Networks for a Single Line-to-Ground Fault at m

At Relay S:

$$V_{2F} = -I_{2S} \cdot (Z_{2S} + m \cdot Z_{2L}) \quad (8)$$

At Relay R:

$$V_{2F} = -I_{2R} \cdot (Z_{2R} + (1-m) \cdot Z_{2L}) \quad (9)$$

Eliminate V_{2F} from Equations 8 and 9 and rearrange the resulting expression as follows:

$$I_{2R} = I_{2S} \cdot \frac{(Z_{2S} + m \cdot Z_{2L})}{(Z_{2R} + (1-m) \cdot Z_{2L})} \quad (10)$$

To avoid alignment of Relay S and R data sets, take the magnitude of both sides of Equation 10 as follows:

$$|I_{2R}| = \left| I_{2S} \cdot \frac{(Z_{2S} + m \cdot Z_{2L})}{(Z_{2R} + (1-m) \cdot Z_{2L})} \right| \quad (11)$$

Equation 11 is then simplified to Equation 12 below.

$$|I_{2R}| = \frac{|(I_{2S} \cdot Z_{2S}) + m \cdot (I_{2S} \cdot Z_{2L})|}{|(Z_{2R} + Z_{2L}) - m \cdot (Z_{2L})|} \quad (12)$$

To further simplify Equation 12, define the following variables:

$$\begin{aligned} I_{2S} \cdot Z_{2S} &= a + jb \\ I_{2S} \cdot Z_{2L} &= c + jd \\ Z_{2R} + Z_{2L} &= e + jf \\ Z_{2L} &= g + jh \end{aligned}$$

Substituting these variables into Equation 12 produces:

$$|I_{2R}| = \frac{|(a + jb) + m \cdot (c + jd)|}{|(e + jf) - m \cdot (g + jh)|} \quad (13)$$

Taking the square of both terms of Equation 13, expanding and rearranging terms produces a quadratic equation of the form:

$$A \cdot m^2 + B \cdot m + C = 0 \quad (14)$$

Equation 14 is solved for m using a quadratic solution. The coefficients of Equation 14 are given below.

$$\begin{aligned} A &= |I_{2R}|^2 \cdot (g^2 + h^2) - (c^2 + d^2) \\ B &= -2 \cdot |I_{2R}|^2 \cdot (e \cdot g + f \cdot h) - 2 \cdot (a \cdot c + b \cdot d) \\ C &= |I_{2R}|^2 \cdot (e^2 + f^2) - (a^2 + b^2) \end{aligned} \quad (15)$$

DISTRIBUTION SYSTEMS

Fault location for distribution feeders uses the same basic principles as for transmission lines, but presents a great challenge for substation fault locators because of the diverse topology of the distribution system: laterals, spurs, and single-phase taps. On important feeders, some utilities model the line parameters to achieve a more precise fault location.

One utility models a feeder using an Excel[®] spreadsheet to show the line parameters. The spreadsheet includes node numbers, wire size, distance from the source, positive- and zero-sequence impedances, and fault currents. Figure 7 is an actual model of a feeder that is 5.47 miles long.

TO NODE Number	FEEDER T2	36384	Source Line	Feet	Miles from Source	Cumulative Per Unit Impedance				Calculated Fault Currents at the end of this branch				Per Unit Impedance for this conductor or Transformer				(Cumulative Line Z Ohms)		Percent Impedance per 1000 feet	
						0.0114 -j 0.2487		0.0080 -j 0.2201		8850 9204 13997 14557		2192		R1 -j X1		R0 -j X0		R1 -j X1		R0 -j X0	
						R1 -j X1	R0 -j X0	R1 -j X1	R0 -j X0	I3	Iph-g	Assg m. I3	Assg m. XPR	R1 -j X1	R0 -j X0	R1 -j X1	R0 -j X0	R1 -j X1	R0 -j X0	R1 -j X1	R0 -j X0
2	CD_28kV_XLPE	750	580	0.5	0.0142	-j 0.2552	0.0294	-j 0.2239	8622	9983	13307	13947	1830	0.0028	0.0064	0.0124	0.0038	0.0020	-j 0.004	0.009	-j 0.003
3	DB_28kV_XLPE	500	2800	0.66	0.0362	-j 0.2753	0.0751	-j 0.2377	7937	8217	10867	11259	759	0.0221	0.0201	0.0547	0.0138	0.0186	-j 0.009	0.282	-j 0.074
4	OH_XARM	336 ACSR	3062	1.24	0.0599	-j 0.3306	0.1380	-j 0.3978	6559	6049	8402	7748	552	0.0236	0.0553	0.0629	0.1601	0.273	-j 0.479	0.609	-j 1.684
5	DB_28kV_XLPE	500	906	1.41	0.0670	-j 0.3271	0.1557	-j 0.4023	6412	5910	8043	7413	500	0.0071	0.0065	0.0177	0.0045	0.307	-j 0.747	0.939	-j 0.85
6	DB_28kV_XLPE	500	1973	1.79	0.0826	-j 0.3512	0.1942	-j 0.4120	6108	5617	7372	6778	425	0.0155	0.0141	0.0385	0.0097	0.527	-j 1.076	1.121	-j 2.285
7	OH_XARM	336 ACSR	2684	2.29	0.1033	-j 0.3997	0.2494	-j 0.5524	5338	4618	6303	5452	387	0.0207	0.0485	0.0551	0.1404	0.560	-j 1.154	1.874	-j 4.823
8	OH_XARM	336 ACSR	649	2.42	0.1083	-j 0.4114	0.2627	-j 0.5963	5180	4427	6090	5296	380	0.0050	0.0117	0.0153	0.0339	1.229	-j 1.535	1.992	-j 6.095
9	OH_XARM	336 ACSR	2096	2.81	0.1245	-j 0.4493	0.3058	-j 0.6359	4727	3906	5493	4539	361	0.0162	0.0379	0.0431	0.1096	0.651	-j 1.369	1.372	-j 5.561
10	OH_XARM	336 ACSR	2506	3.29	0.1438	-j 0.4945	0.3572	-j 0.8270	4279	3424	4919	3936	344	0.0193	0.0453	0.0515	0.1311	0.668	-j 1.409	1.405	-j 5.732
11	OH_XARM	336 ACSR	1577	2.56	0.1135	-j 0.4246	0.2777	-j 0.6244	5015	4231	5869	4953	375	0.0106	0.0249	0.0283	0.0720	0.852	-j 1.843	1.777	-j 7.524
12	OH_XARM	336 ACSR	4025	7	0.1344	-j 0.4724	0.3321	-j 0.7629	4487	3644	5184	4210	352	0.0311	0.0727	0.0827	0.2105	0.895	-j 1.734	1.683	-j 7.147
13	OH_XARM	336 ACSR	1115	3.27	0.1617	-j 0.4958	0.3809	-j 0.8395	4226	3371	4739	3789	307	0.0273	0.0234	0.0489	0.0726	0.863	-j 1.870	1.804	-j 7.742
14	OH_XARM	336 ACSR	861	3.24	0.1418	-j 0.4698	0.3518	-j 0.8131	4322	3469	4974	3952	345	0.0074	0.0174	0.0197	0.0503	0.955	-j 1.898	1.586	-j 8.878
15	DB_28kV_XLPE	500	778	3.39	0.1479	-j 0.4953	0.3670	-j 0.8170	4263	3426	4872	3916	335	0.0061	0.0056	0.0152	0.0038	0.708	-j 1.504	1.487	-j 6.146
16	OH_XARM	336 ACSR	1459	3.68	0.1592	-j 0.5217	0.3970	-j 0.8933	4040	3196	4596	3636	328	0.0113	0.0264	0.0300	0.0763	0.824	-j 1.777	1.720	-j 7.334
17	OH_XARM	336 ACSR	1129	3.88	0.1679	-j 0.5421	0.4201	-j 0.9523	3893	3030	4403	3445	323	0.0087	0.0204	0.0232	0.0590	0.891	-j 1.934	1.905	-j 8.020
18	OH_XARM	336 ACSR	578	3.99	0.1724	-j 0.5525	0.4320	-j 0.9825	3807	2963	4310	3395	321	0.0045	0.0104	0.0119	0.0302	0.971	-j 2.124	2.018	-j 8.845
19	OH_XARM	336 ACSR	412	16	0.1624	-j 0.5291	0.4054	-j 0.9148	3981	3137	4523	3564	326	0.0032	0.0074	0.0095	0.0215	1.131	-j 2.500	2.240	-j 10.494
20	OH_XARM	336 ACSR	3950	4.47	0.1921	-j 0.5987	0.4845	-j 1.1162	3008	2672	3944	3087	312	0.0297	0.0636	0.0791	0.2014	1.202	-j 2.668	2.672	-j 10.928
21	OH_XARM	336 ACSR	4834	5.39	0.2294	-j 0.6860	0.5838	-j 1.3690	3046	2252	3399	2513	299	0.0373	0.0873	0.0993	0.2528	1.294	-j 2.649	2.745	-j 10.588
22	OH_XARM	336 ACSR	2735	4.99	0.2132	-j 0.6401	0.5407	-j 1.2592	3230	2417	3616	2706	304	0.0211	0.0494	0.0562	0.1430	1.330	-j 2.682	2.835	-j 10.608
23	OH_XARM	336 ACSR	2571	5.47	0.2331	-j 0.6945	0.5935	-j 1.3937	3006	2218	3393	2473	296	0.0159	0.0464	0.0528	0.1345	1.396	-j 2.707	2.904	-j 10.626

Figure 7 Spreadsheet Model (See Appendix for Enlarged View)

A graphical representation of the feeder is shown in Figure 8.

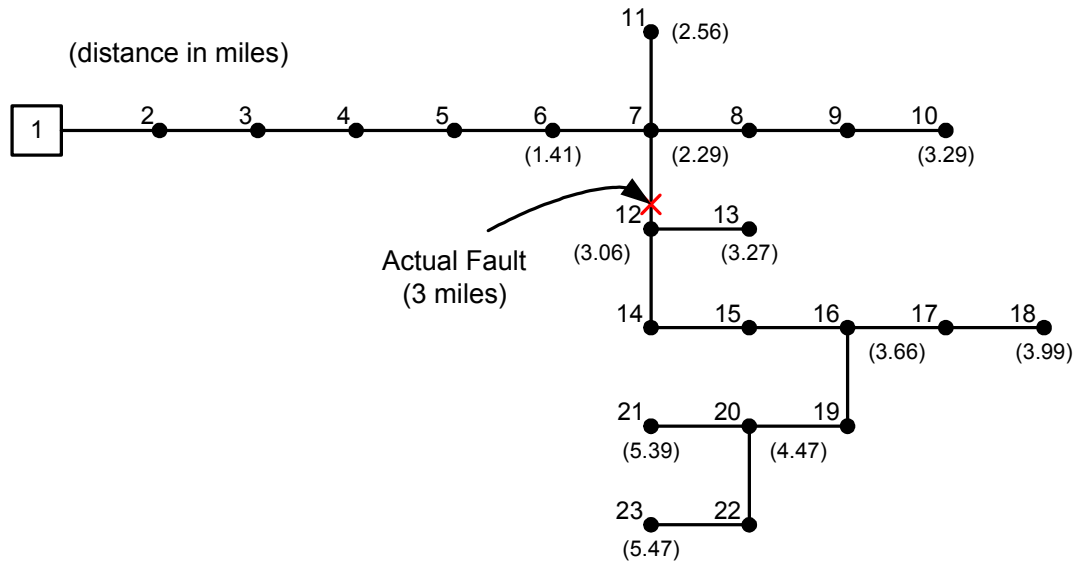


Figure 8 Distribution Feeder Topology

Figure 9 shows a screen capture of event report data from an actual fault.

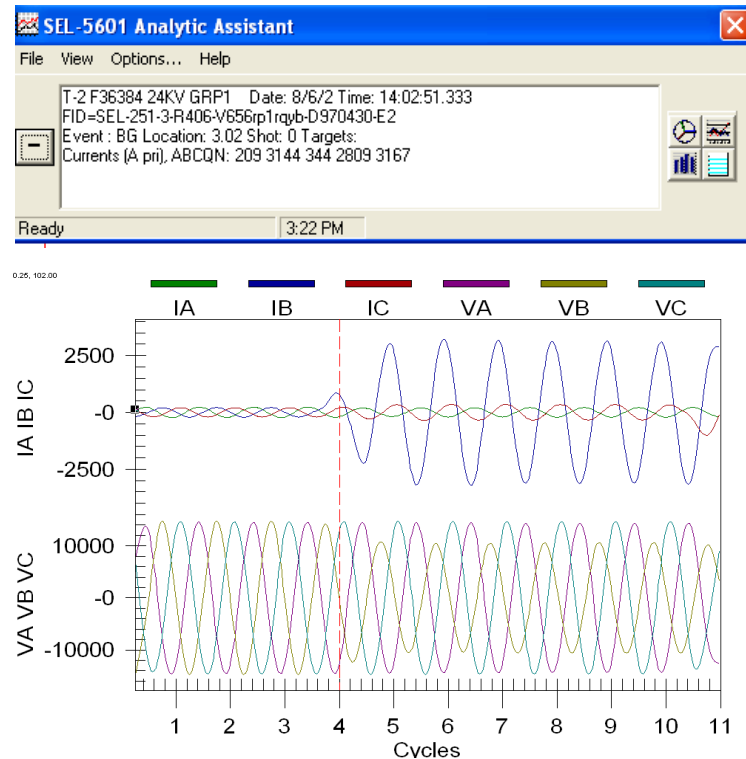


Figure 9 Distribution Feeder Fault Event Screen Capture

The event report indicates that a B-phase-to-ground fault occurred 3.02 miles from the station. From the feeder topology, there are two possible locations for the fault. As it turns out, line crews found a fast growing skinny tree growing close to the line, approximately three miles from the substation on the main line near Node 12.

USE OF FAULT INDICATORS

Fault Indicators can be applied on lines to help locate faults. If a fault occurs beyond the location of the fault indicator, line crews observe an LED or flashing light, indicating that fault current was sensed. Reset can be done manually, electrostatically, or through a timer, depending on the design. Figure 10 is an example of how fault indicators can be placed to assist line crews in finding the fault location.

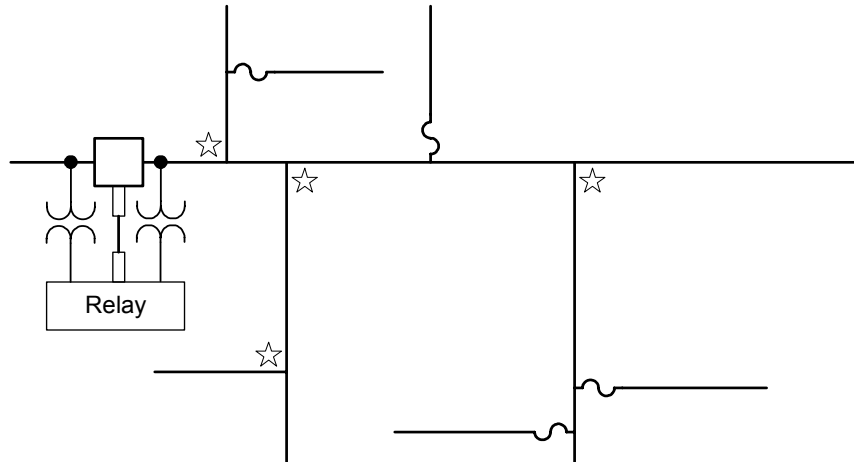


Figure 10 Example Location for Fault Indicators on Distribution Feeder

TRANSMISSION FAULT LOCATION EXAMPLES

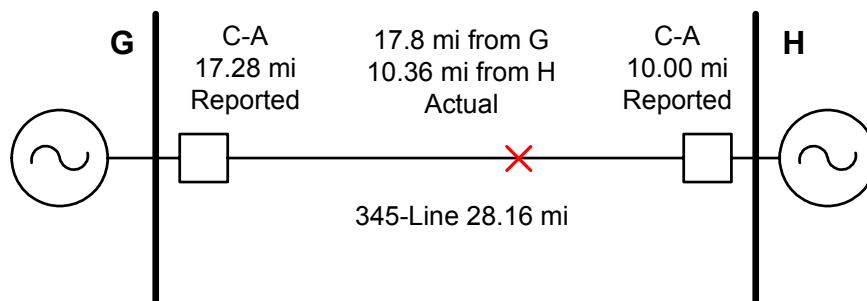
Example 1: 345 kV Automatic Spraying System

Background: Repeated phase-phase faults had occurred on a 345 kV line. There was no inclement weather or lightning in the area. The number of faults caused voltage issues and a negative-sequence overcurrent element went into an alarm state at a regional nuclear plant. Nuclear plant personnel were concerned about the possibility of tripping the unit off line.

The line data for the transmission line:

- Circuit 345-LINE is a 28.16 mile long, 345kV line between terminals G and H.
- 345-LINE—“We had dispatched linemen to the area based on fault location. The lineman was patrolling the line in the area when he observed an automatic spraying system operating very near the line. He went to the property owner’s home and learned that the automatic system runs along a track and sprays liquefied manure onto the open fields. The landowner checked the mechanism that controls the sprinkler and found that it had failed, causing the sprinkler to run under the line.”

Figure 11 shows a one-line and event report screen captures.



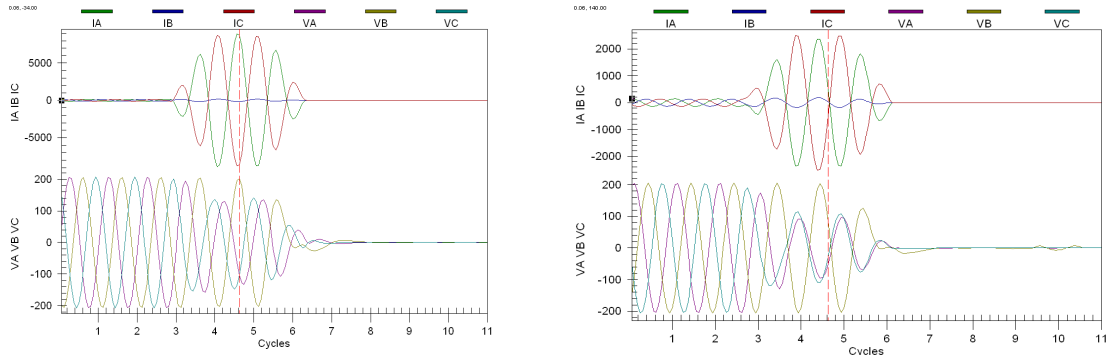


Figure 11 Example 1: One-Line and Event Report Screen Captures

As a way of confirming that the data was correct, we ran the two-ended negative-sequence impedance algorithm using the event reports from each end, as shown in Figure 12.

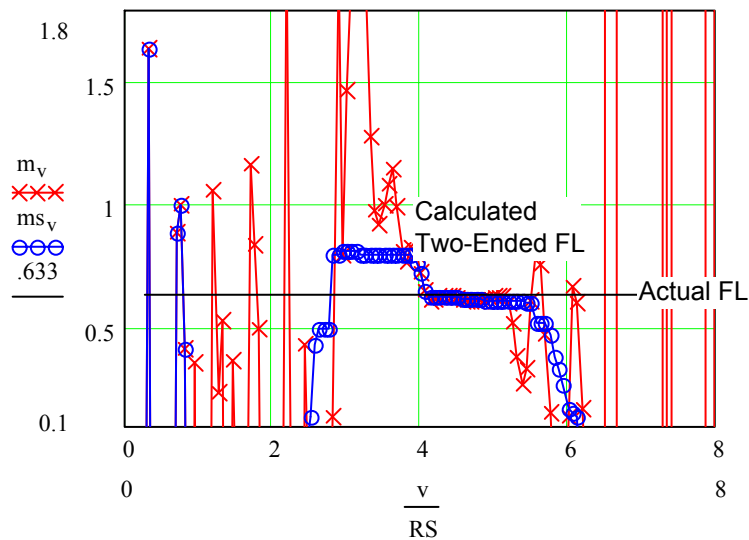


Figure 12 Example 1: Mathcad Screen Capture—Actual Fault Location vs. Two-Ended Estimate

The actual fault occurred where the sprinkler system was found, between 17.8 and 17.9 miles ($m = .633$) from Terminal G (based on patrol map tower locations).

Conclusions for Example 1:

1. The one-ended (17.28 and 10.00 miles, respectively) and two-ended (17.46 miles) fault locations yielded good results. All fault location estimates were within 2%.
2. Two-ended negative-sequence impedance-based method corroborates one-ended method.

Example 2: Incorrect Fault Location Due to Incorrect Fault Type Identified

Background: On this 115 kV Line, a relay tripped for an apparent fault. Targets indicated an A-B fault that tripped on Zone 2. Upon analysis of the event report data, both ground directional overcurrent and ground distance elements tripped. All of the data indicated that the

relay elements functioned properly. However, the relay produced a fault location estimate of -143 miles. This spawned an investigation to find the correct fault location.

Figure 13 shows a one-line and event report screen captures.

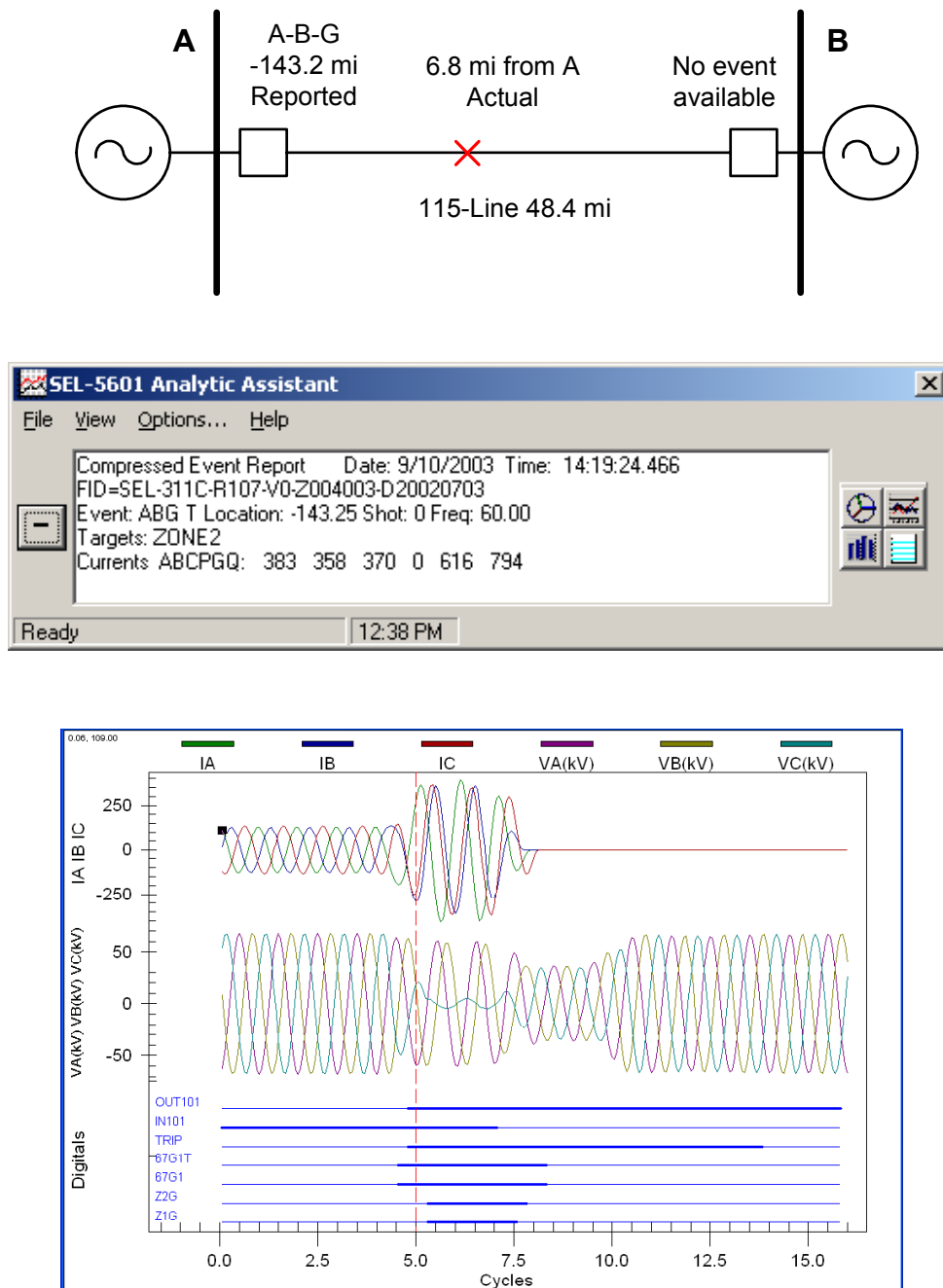


Figure 13 Example 2: One-Line and Event Report Screen Captures

By inspecting the event data directly, we saw a depressed C-phase to ground voltage and relatively low fault current (under 400 A primary) on all three phases. Based on this, we suspected that the fault was C-phase to ground with a weak source behind the relay and that the relay selected the wrong fault type.

The relay used in this application is for three-pole trip applications. Its fault identification logic compares the angular relationship between I_0 and I_2 [5]. For this fault, I_2 leads I_0 by about 120 degrees (using A-phase as reference), as shown in Figure 14. This indicates that the fault is either C-phase to ground, or A-B-ground.

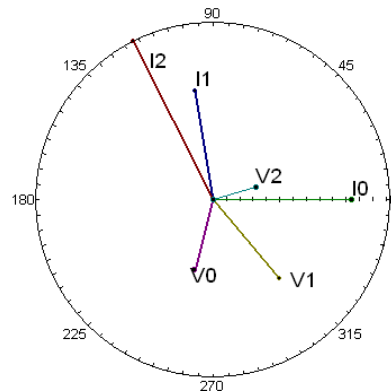


Figure 14 Symmetrical Components from Fault— I_2 leads I_0 by 120 degrees

The relay then performs “torque” calculations to determine which fault appears to be “closer” to the relay to decide between the two loops (C-G or A-B-G). For this case, the “torque” calculation showed the A-B-G as being closest. Thus, the relay selected the wrong loop.

Improved relay designs (intended for single-pole or three-pole applications) have better fault-type selection. These designs measure the fault resistance between phases and phase-to-ground. These would have correctly identified the fault type.

Still, this example demonstrates the need for correct fault type selection. Knowing that the fault was C-G or A-B-G, we calculated the actual fault location to be 6.8 miles for the C-phase-to-ground fault (calculations from the event report data using the one-ended modified Takagi method):

Calculated Fault Locations:

C-G: 6.8 A-B-G: -137

Conclusions for Example 2:

1. Fault was C-phase-to-ground, one-ended location 6.8 miles. (later confirmed from field reports).
2. Weak source conditions challenge the one-ended fault locators for two reasons: nonhomogeneous system is more likely; fault type selection more difficult.
3. Superior fault type selection would have provided the correct fault type and fault location.
4. Two-ended negative-sequence impedance fault location would have correctly selected fault location for faults all along the line. (fault type selection not needed)

Example 3: 345 kV Line Failed Insulator

The line data for the transmission line:

- Circuit 345-LINE is a 39.26 mile long, double-circuit 345 kV line between terminals E and F.

- 345-LINE circuit fault data:
 - 345-LINE E SUB SEL-311C 08-19-03.txt
 - 345-LINE F SUB SEL-311C 08-19-03.txt
- 345-LINE – “A failed insulator strut was found on structure # 483, at about 6 miles from the F termination. Total line length is 39.26 miles.” *Note – the line length setting in the relays is 39.30 miles.*

Figure 15 shows a one-line and event report screen captures.

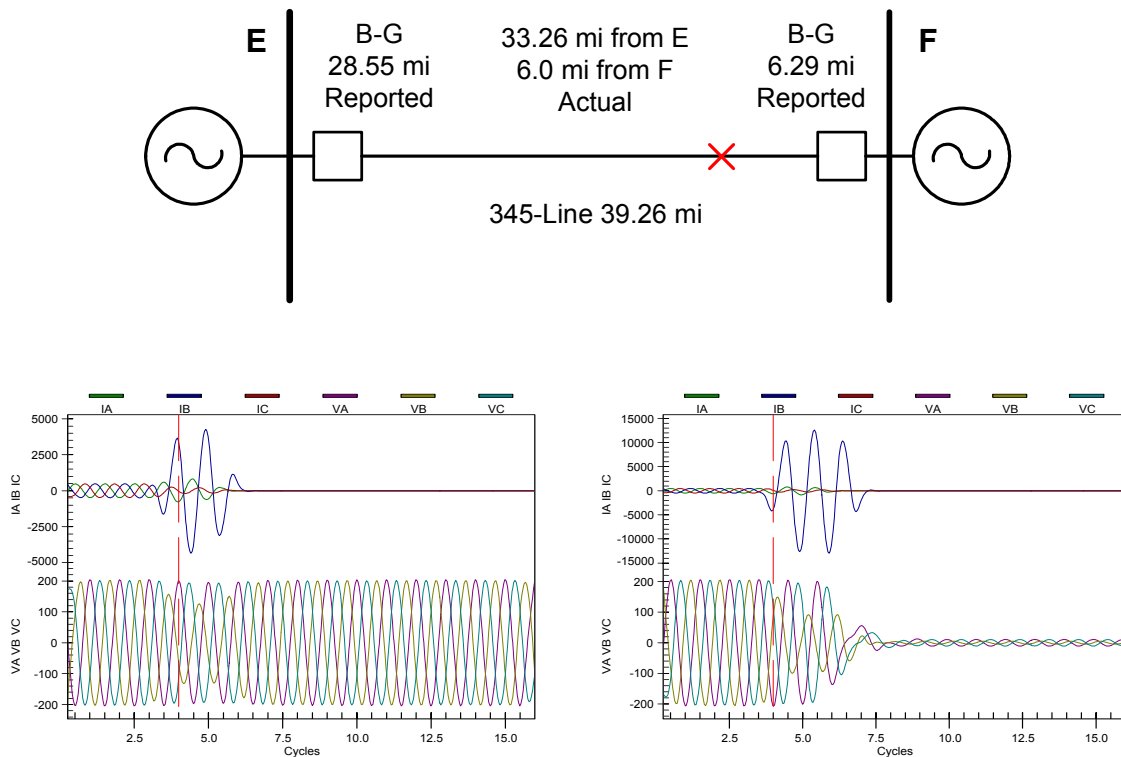


Figure 15 Example 3: One-Line and Event Report Screen Captures

In Figure 16, the horizontal axis is the number of cycles and the vertical axis is the two-ended fault location averaged over several cycles. The actual fault location (33.26 miles) is about 0.85 per unit from the E terminal (depicted by a horizontal line on the graph). Note that the calculated fault locations are close to but do not exactly match the actual.

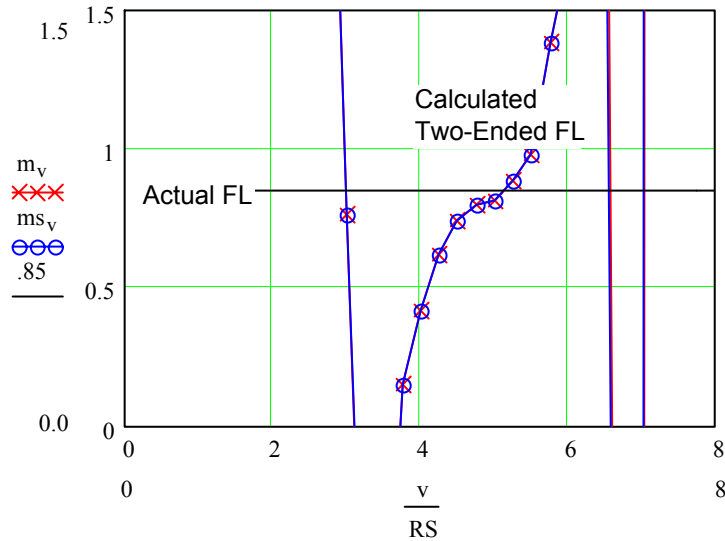


Figure 16 Example 3: Mathcad Screen Capture—Actual Fault Location versus Two-Ended Estimate

Conclusions for Example 3:

1. The system was slightly nonhomogeneous, which contributed to the poor local one-ended fault location estimate and the remote end being more accurate.
2. The fault was a fast clearing fault (approximately two cycles). The fault was interrupted just as the relay filtering (one-cycle cosine filter) had processed the data. As a result, fault location results are based on data less accurate than that of a fault present for a longer time window.
3. The only event reports collected were 4-sample per cycle event reports. Thus, our analysis was limited because of the limited number of data points. When possible, it is better to collect event data with more data points (16 or more samples-per-cycle).
4. Two-ended negative-sequence impedance fault location provided the best estimate, mainly because it mitigated any effects of the nonhomogeneous system and smoothed out the short data window by averaging the fault location estimates over several samples.

Example 4 - 345 kV Line – Fire Under Line Conductors

Background: There was a fire on a long 345 kV line in a wooded area. The fire caused several faults to occur, on different phases. Several reclose attempts were momentarily successful, until the still burning fire caused other phases to flash over creating another fault.

- 345-LINE – “Line crews found a fire burning under a transmission line approximately 90.7 miles from the G substation. Total line length is 160.63 miles.”

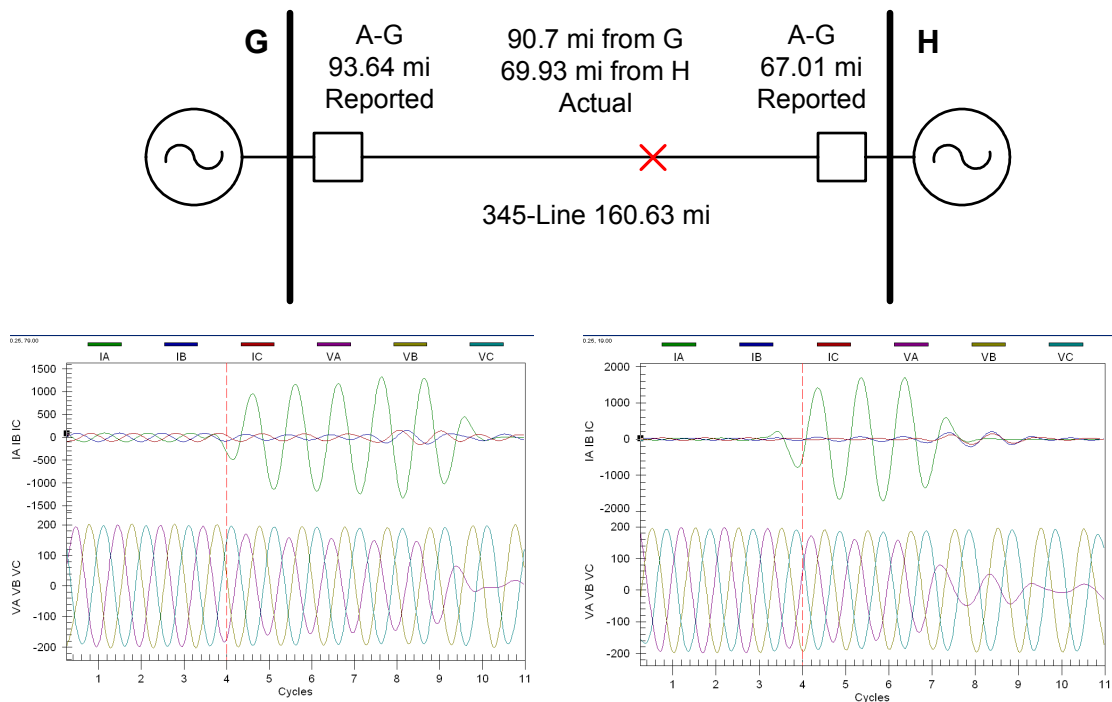


Figure 17 Example 4: One-Line and Event Report Screen Captures

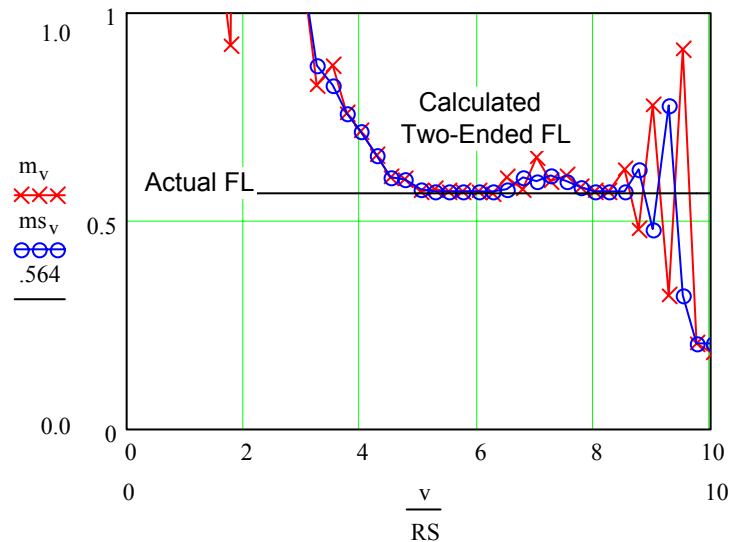


Figure 18 Example 4: MathCad Screen Capture—Actual Fault Location vs Two-Ended Estimate

Conclusions for Example 4:

In Figure 18, the horizontal axis is the number of cycles and the vertical axis is the two-ended fault location averaged over several cycles. The actual fault location (90.7 miles) is 0.564 per unit from the G terminal (depicted by a horizontal line on the graph). Even though the one-ended

method produced good results, the two-ended negative-sequence impedance method is superior and allows operators to get much closer to the actual fault location.

LAB TESTS TO OBTAIN TWO-ENDED FAULT LOCATION FROM ONE END

The examples from the previous sections show how we can use the two-ended negative-sequence impedance method to get fault location data for operators. However, it takes time to collect the event reports and analyze the data. Is there any way we can get the two-ended data faster?

Many relays have the capability to send and receive the status of up to eight digital elements. In some newer designs, if less than 8 bits are used, we can use the unassigned bits to send additional information, such as remote time synchronization, virtual terminal sessions, and analog data.

Via relay settings, we can send either measured or calculated analog quantities over a communication channel. Remembering that we need to exchange negative-sequence impedance and current information, we made an effort in the lab to calculate two-ended fault location from a single end with some promising results.

Once analog values are sent, the remote relay receives the analog quantities. The received analog quantities can be used directly in logic or math equations and viewed using a software command.

The relay receiving the remote data then processes the multi-ended fault location algorithm. To do this, the relay uses internal mathematical capabilities, such as trigonometric functions, multiplication, division, addition, subtraction, and square root, to solve the quadratic equation for the fault location.

LAB TEST SETUP

Several line faults with known fault locations were used as test cases. Local and remote relays exchange and use fault data for the purpose of implementing the two-ended negative-sequence impedance fault location algorithm.

We created a time-aligned COMTRADE file from the two line-end event reports for each fault. This fault simulation file is replayed into two relays to simulate the faults as seen by the relays in the field.

The relays measure phase currents and voltages, and calculate $3I_2$ and ZS_2 . The magnitude of $3I_2$, and the magnitude and angle of ZS_2 from the remote line terminal is needed by the local relay to calculate a two-ended fault location. Therefore, we have to first save the $3I_2$ and ZS_2 values at an appropriate time during the fault, and then communicate those values to the remote line terminal for the purpose of the fault location calculation.

The data from the two ends of the line does not have to be time-aligned. However, we do need to select a point during the fault when values have settled to a steady state. We arbitrarily chose a point 1.5 cycles after fault detection for our data capture. At that point in time, the local relays will lock and hold the present fault value of $3I_2$ and ZS_2 . These values are sent to the remote line terminal. The remote line terminal will then perform a two-ended fault algorithm.

Once physical test connections are verified and data scaled properly, the fault is played back to the relays. We compared the actual event report data to the played back data to verify accuracy, as shown in Figure 19.

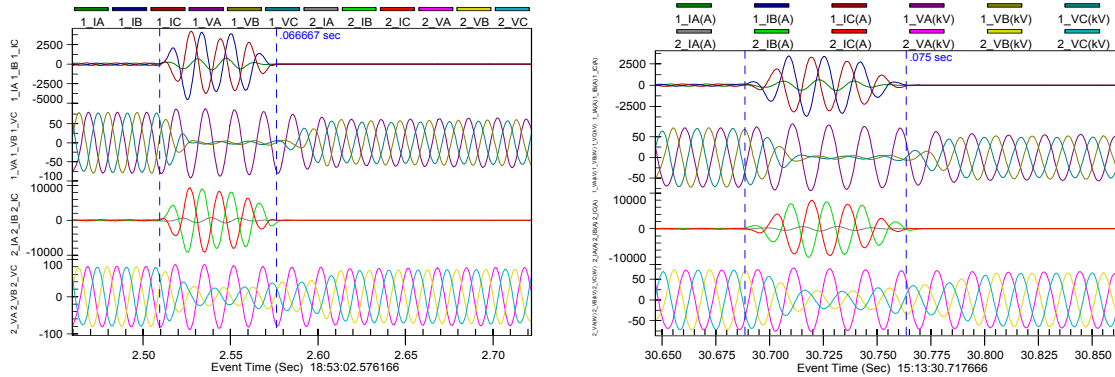


Figure 19 Screen Capture of Original Event Data and COMTRADE Event Data

TEST RESULTS AND ANALYSIS

Table 2 shows the results from the laboratory tests.

Table 2 Results From 345 kV Line Fault Location Lab Tests

Case Study	Actual Location	One-Ended Estimate		Two-Ended Estimate		
		(Local)	(Remote)	Mathcad Point	Mathcad Average	Relay
345-LINE Example 2	90.7 miles	93.64 miles	67.01	91.2 miles	90.7 miles	91.25 miles

The One-Ended Estimate is the fault location taken directly from the relays.

The Two-Ended Mathcad Point Estimate is a fault location based on the two-ended negative-sequence impedance method, where two-ended event report data are manually entered from one point in time (selected by the user).

The Two-Ended MathCad Average Estimate is based on the two-ended negative-sequence impedance method that averages the fault location over several samples. These results are produced using four-samples-per-cycle event reports.

The Two-Ended Relay Estimate is the two-ended negative-sequence impedance fault location automatically estimated by a relay using local and remote data captured 1.25 or 1.5 cycles after fault inception. (This estimate is based on the Two-Ended Mathcad Point Estimate Method.) A detailed listing of the logic settings and calculated analog results are in the Appendix.

CONCLUSIONS

1. One-ended impedance-based fault location still produces very good results in most cases.
2. If event data are available from both ends of the line, two-ended impedance fault location can improve fault location estimate.
3. Off-line analytical tools are available to find the best fault location estimates.

4. Improve results by collecting events with the highest sampling rate and by using the average of several fault location estimate samples instead of a single point estimate.
5. Short events present a challenge. More analysis is often required to get a more accurate fault estimate because of the short data window. The longer an event lasts, the better the fault location estimate.
6. Technology is available to automatically calculate a two-ended fault location from a single end. Lab testing confirmed the viability of the technology. Testing indicates that accuracy is good on stable, longer lasting events.
7. Developments are needed to make automatic collection of two-ended fault location applicable for all lines and faults.

REFERENCES

- [1] IEEE Standard PC37.114, "Draft Guide For Determining Fault Location on AC Transmission and Distribution Lines," 2004.
- [2] T. Takagi, Y. Yamakoshi, M. Yamaura, R. Kondou, and T. Matsushima, "Development of a New Type Fault Locator Using the One-Terminal Voltage and Current Data," IEEE Transactions on Power Apparatus and Systems, Vol. PAS-101, No. 8, August 1982, pp. 2892-2898.
- [3] Edmund O. Schweitzer, III, "A Review of Impedance-Based Fault Locating Experience," Proceedings of the 15th Annual Western Protective Relay Conference, Spokane, WA, October 24-27, 1988.
- [4] D.A. Tziouvaras, J.B. Roberts, G. Benmouyal, "New Multi-Ended Fault Location Design For Two- or Three-Terminal Lines," presented at CIGRE Conference, 1999, <http://www.selinc.com/techpprs/6089.pdf>.

BIOGRAPHIES

David Costello graduated from Texas A&M University in 1991 with a BSEE. He worked as a System Protection Engineer for Central and Southwest, and served on the System Protection Task Force for the ERCOT. In 1996, David joined Schweitzer Engineering Laboratories, where he has served as a Field Application Engineer and Regional Service Manager. He presently holds the title of Senior Application Engineer and works in Boerne, Texas. He is a member of IEEE, and the Planning Committee for the Conference for Protective Relay Engineers at Texas A&M University.

Karl Zimmerman is a Senior Application Engineer with Schweitzer Engineering Labs in Belleville, Illinois. His work includes providing application support and technical training for protective relays. He is an active member of the IEEE Power System Relaying Committee and is the Chairman of Working Group D-2 on fault locating. Karl received his BSEE degree at the University of Illinois at Urbana-Champaign and has over 20 years of experience in the area of system protection. He is a past speaker at many technical conferences and has authored several papers and application guides on protective relaying.

APPENDIX

The following are the relay logic settings to perform two-ended fault location from one end after receiving data from remote terminal. We based these settings on the two-ended negative-sequence impedance fault location method described in this paper.

```
=>>SHO L
Protection 1
1: #
2: # THESE SETTINGS ARE USED FOR TWO-ENDED FAULT LOCATION
3: #
4: # USE DEFINITE-TIME O/C DELAYS IN CONJUNCTION WITH
5: # A COND TIMER TO MARK 1.5 CYCLES INTO FAULT
6: #
7: PCT10PU := 0.000000
8: PCT10D0 := 0.875000 #1.0 CYCLE DELAY INCLUDING PROCESSING TIME
9: PCT10IN := R_TRIG 67P1T OR R_TRIG 67G1T
10: #
11: # USE A PROCESSING-INTERVAL WIDE PULSE TO MARK THE FAULT DATA
12: #
13: PSV02 := F_TRIG PCT10Q # 2 MSEC PULSE 1.5 CYCLES AFTER EVENT TRIGGER
14: PSV03 := NOT PSV02 # THIS WILL BE ONE ALL TIMES EXCEPT DURING FAULT
15: #
16: # MEMORIZE FAULT DATA I2S MAG & ANG, Z2S MAG AND ANG, V2S MAG AND ANG
17: # READ MEASURED VALUE TIMES PULSE BINARY ONE DURING FAULT, PLUS ZERO
18: # NEXT TIME THRU, READ ZERO PLUS PREVIOUS STORED VALUE TIMES ONE
19: #
20: PMV01 := L3I2FIM * PSV02 + PMV01 * PSV03
21: # PMV01 STORES THE LINE 3I2 MAGNITUDE AT 1.5 CYCLES AFTER EVENT TRIGGER
22: # UNTIL A NEW EVENT OCCURS
23: #
24: PMV02 := L3I2FIA * PSV02 + PMV02 * PSV03
25: # PMV02 STORES THE LINE 3I2 ANGLE AT 1.5 CYCLES AFTER EVENT TRIGGER
26: # UNTIL A NEW EVENT OCCURS
27: #
28: PMV03 := 3V2FIM * PSV02 + PMV03 * PSV03
29: # PMV03 STORES THE LOCAL 3V2 MAGNITUDE AT 1.5 CYCLES AFTER EVENT
30: # TRIGGER UNTIL A NEW EVENT OCCURS
31: #
32: PMV04 := 3V2FIA * PSV02 + PMV04 * PSV03
33: # PMV04 STORES THE LOCAL 3V2 ANGLE AT 1.5 CYCLES AFTER EVENT
34: # TRIGGER UNTIL A NEW EVENT OCCURS
35: #
36: PMV05 := (3V2FIM / (L3I2FIM + 0.001000)) * PSV02 + PMV05 * PSV03
37: # PMV05 STORES THE NEG SEQ SOURCE IMPEDANCE MAGNITUDE AT 1.5 CYCLES
38: # AFTER EVENT TRIGGER UNTIL A NEW EVENT OCCURS
39: #
40: PMV06 := (3V2FIA - L3I2FIA) * PSV02 + PMV06 * PSV03
41: # PMV06 STORES THE NEG SEQ SOURCE IMPEDANCE ANGLE AT 1.5 CYCLES AFTER
42: # EVENT TRIGGER UNTIL A NEW EVENT OCCURS
43: #
44: # ANALOG MIRRORED BIT VALUES ARE 16-BIT SIGNED INTEGERS
45: # SO WE MUST SCALE APPROPRIATELY BEFORE SENDING TO RETAIN ACCURACY
46: #
47: PMV07 := PMV01 * 100.000000 # SCALE 3I2 MAG BY MULTIPLYING BY 100
48: PMV08 := PMV05 * 100.000000 # SCALE Z2S MAG BY MULTIPLYING BY 100
49: PMV09 := PMV06 * 10.000000 # SCALE Z2S ANGLE BY MULTIPLYING BY 10
50: #
51: # SEND PMV07, PMV08, AND PMV09 AS MIRRORED BIT ANALOGS
52: # AND REMEMBER TO DIVIDE BY SCALING VALUE AT OTHER END
53: #
54: PMV10 := 0.970000 # ENTER Z1MAG FROM RELAY SETTINGS HERE
55: PMV11 := 79.000000 # ENTER Z1ANG FROM RELAY SETTINGS HERE
```

```

56: PMV12 := 2.170000 # ENTER LINE LENGTH FROM RELAY SETTINGS HERE
57: #
58: # SCALE RECEIVED MIRRORED BIT ANALOG VALUES FROM REMOTE RELAY
59: #
60: PMV13 := MB1A / 100.000000 # REMOTE 3I2 MAG RECEIVED THRU MB A, SCALED
61: PMV14 := MB2A / 100.000000 # REMOTE Z2S MAG RECEIVED THRU MB A, SCALED
62: PMV15 := MB3A / 10.000000 # REMOTE Z2S ANGLE RECEIVED THRU MB A, SCALED
63: #
64: # CORRECTION MADE - CONVERT TO PRIMARY VALUES
65: #
66: # NEXT WE SOLVE THE QUADRATIC EQUATION AND DETERMINE FAULT LOCATION
67: # REFER TO ROBERTS, TZIOUVARAS, BENMOUYAL "NEW MULTI-ENDED FAULT LOC"
68: # REFER TO MOXLEY, WOODWARD "IMPROVE SUBSTATION CONTROL AND PROTECTION"
69: # REFER TO ZIMMERMAN "TWO-ENDED FAULT LOCATION" MATHCAD FILE
70: #
71: PMV16 := (PMV03 * 600.000000 / 3.000000) * COS(PMV04) # A'
72: PMV16 := (PMV03 * 600.000000 / 3.000000) * COS(PMV04) # A'
73: PMV17 := (PMV03 * 600.000000 / 3.000000) * SIN(PMV04) # B'
74: #
75: PMV18 := (PMV01 * 400.000000 / 3.000000) * (PMV10 * 600.000000 / \
400.000000)
76: PMV18 := PMV18 * COS(PMV02 + PMV11) # C'
77: #
78: PMV19 := (PMV01 * 400.000000 / 3.000000) * (PMV10 * 600.000000 / \
400.000000)
79: PMV19 := PMV19 * SIN(PMV02 + PMV11) # D'
80: #
81: PMV20 := (PMV14 * 600.000000 / 400.000000) * COS(PMV15)
82: PMV20 := PMV20 + (PMV10 * 600.000000 / 400.000000) * COS(PMV11) # E'
83: #
84: PMV21 := (PMV14 * 600.000000 / 400.000000) * SIN(PMV15)
85: PMV21 := PMV21 + (PMV10 * 600.000000 / 400.000000) * SIN(PMV11) # F'
86: #
87: PMV22 := (PMV10 * 600.000000 / 400.000000) * COS(PMV11) # G'
88: #
89: PMV23 := (PMV10 * 600.000000 / 400.000000) * SIN(PMV11) # H'
90: #
91: PMV24 := (PMV13 * 400.000000 / 3.000000) * (PMV13 * 400.000000 / \
3.000000) * (PMV22 * PMV22 + PMV23 * PMV23)
92: PMV24 := PMV24 - (PMV18 * PMV18 + PMV19 * PMV19)
93: # PREVIOUS LINE IS A
94: #
95: PMV25 := -2.000000 * (PMV13 * 400.000000 / 3.000000) * (PMV13 * \
400.000000 / 3.000000)
96: PMV25 := PMV25 * (PMV20 * PMV22 + PMV21 * PMV23)
97: PMV37 := PMV25 - 2.000000 * (PMV16 * PMV18 + PMV17 * PMV19)
98: # PREVIOUS LINE IS B - NOTE EQUATION STARTS WITH "-2"
99: # CORRECTING A TYPOGRAPHICAL ERROR IN REFERENCES ABOVE
100: #
101: PMV26 := (PMV13 * 400.000000 / 3.000000) * (PMV13 * 400.000000 / \
3.000000) * (PMV20 * PMV20 + PMV21 * PMV21)
102: PMV26 := PMV26 - (PMV16 * PMV16 + PMV17 * PMV17)
103: # PREVIOUS LINE IS C
104: #
105: PMV27 := ABS(PMV37 * PMV37 - 4.000000 * PMV24 * PMV26)
106: PMV27 := SQRT(PMV27)
107: PMV27 := PMV27 - PMV37
108: PMV28 := PMV27 * PMV12 / (2.000000 * (PMV24 + 0.001000))
109: # PREVIOUS LINE IS M1 FAULT LOC ESTIMATE
110: #
111: PMV29 := -PMV37
112: PMV30 := (PMV37 * PMV37 - 4.000000 * PMV24 * PMV26)
113: PMV30 := SQRT(PMV30)
114: PMV31 := -PMV30
115: PMV32 := PMV29 + PMV31
116: PMV33 := PMV32 * PMV12 / (2.000000 * (PMV24 + 0.001000))

```

```

117: # PREVIOUS LINE IS M2 FAULT LOC ESTIMATE
118: #
119: # ONE ESTIMATE WILL BE "REASONABLE", WITHIN THE LINE, TRASH OTHER
120: PMV34 := ABS(PMV28)
121: PSV04 := PMV34 > PMV12
122: PSV05 := NOT PSV04 # THIS WILL BE A LOGICAL ONE IF M1 IS OK
123: PMV35 := ABS(PMV33)
124: PSV06 := PMV35 > PMV12
125: PSV07 := NOT PSV06 # THIS WILL BE A LOGICAL ONE IF M2 IS OK
126: #
127: PMV36 := PSV05 * PMV34 + PSV07 * PMV35 # THIS IS THE FAULT LOC ESTIMATE
128: PMV64 := PMV36 # MOVE FAULT LOC TO AREA VISIBLE TO "METER PMV"
129: #

```

The following shows the analog math results from the relay logic. PMV64 is the two-ended fault location calculated from the relay.

```

=>>>MET PMV A

```

```

4XX RELAY
SUB C

```

```

Date: 09/10/2004 Time: 17:49:07.559
Serial Number: 2004104018

```

Protection Analog Quantities

```

PMV01 = 9.051
PMV02 = -64.952
PMV03 = 14.069
PMV04 = -175.743
PMV05 = 1.554
PMV06 = -110.791
PMV07 = 905.150
PMV08 = 155.413
PMV09 = -1107.905
PMV10 = 3.960
PMV11 = 84.000
PMV12 = 160.630
PMV13 = 11.590
PMV14 = 1.080
PMV15 = 255.700
PMV16 = -14029.924
PMV17 = -1044.396
PMV18 = 33881.355
PMV19 = 11697.921
PMV20 = 3.679
PMV21 = 72.294
PMV22 = 10.348
PMV23 = 98.458
PMV24 = 8.217E+08
PMV25 = -3.076E+09
PMV26 = 9.283E+08
PMV27 = 3.268E+09
PMV28 = 319.442
PMV29 = 2.101E+09
PMV30 = 1.167E+09
PMV31 = -1.167E+09
PMV32 = 9.336E+08
PMV33 = 91.249
PMV34 = 319.442
PMV35 = 91.249
PMV36 = 91.249
PMV37 = -2.101E+09
PMV38 = 0.000
PMV39 = 0.000

```


PMV40	=	3000.000
PMV41	=	120.000
PMV42	=	0.000
PMV43	=	0.000
PMV44	=	0.000
PMV45	=	0.000
PMV46	=	0.000
PMV47	=	0.000
PMV48	=	0.000
PMV49	=	0.000
PMV50	=	0.000
PMV51	=	0.000
PMV52	=	0.000
PMV53	=	0.000
PMV54	=	0.000
PMV55	=	0.000
PMV56	=	0.000
PMV57	=	0.000
PMV58	=	0.000
PMV59	=	0.000
PMV60	=	0.000
PMV61	=	0.000
PMV62	=	0.000
PMV63	=	0.000
PMV64	=	91.249

TO NODE Number	FEEDER T2	36384	Source Line - Wire Size	Miles from FPO Source	Cumulative Per Unit Impedance				Calculated Fault Currents at the end of this branch				Per Unit Impedance for this conductor or Transformer				(Cumulative Line Z Ohms)				Percent Impedance per 1000 feet				
					R1 +jX1	R0 +jX0	R1 +jX1	R0 +jX0	I3	Iph-g m, 13	Assg m, 13	XFR	R1 +jX1	R0 +jX0	R1 +jX1	R0 +jX0	R1 +jX1	R0 +jX0	R1 +jX1	R0 +jX0					
1					0.0114 +j0.2487	0.0080 +j0.2201	0.0080 +j0.2201	0.0080 +j0.2201	8350	3204	13957	14597	2132												
2	CD_28kV_XLPE	750	530	0.13	0.0142 +j0.2552	0.0204 +j0.2239	0.0204 +j0.2239	0.0204 +j0.2239	8622	8993	13387	13947	18.00	0.0028	0.0064	0.0124	0.0038	0.0024	0.0038	0.0024	0.0038	0.0024	0.0038	0.0024	0.0038
3	DE_28kV_XLPE	500	2800	0.66	0.0362 +j0.2753	0.0751 +j0.2377	0.0751 +j0.2377	0.0751 +j0.2377	7937	8217	10857	11250	7.89	0.0221	0.0201	0.0547	0.0138	0.0138	0.0547	0.0138	0.0138	0.0547	0.0138	0.0138	0.0547
4	OH_XARM	336 ACSR	3662	1.24	0.0599 +j0.3396	0.1390 +j0.3978	0.1390 +j0.3978	0.1390 +j0.3978	6359	6049	8402	7748	5.62	0.0236	0.0553	0.0629	0.0501	0.0501	0.0629	0.0501	0.0501	0.0629	0.0501	0.0501	0.0629
5	DE_28kV_XLPE	500	906	1.41	0.0670 +j0.3371	0.1597 +j0.4023	0.1597 +j0.4023	0.1597 +j0.4023	6112	5910	8043	7413	5.03	0.0071	0.0063	0.0177	0.0045	0.0045	0.0177	0.0045	0.0045	0.0177	0.0045	0.0045	0.0177
6	DE_28kV_XLPE	500	1973	1.73	0.0625 +j0.3512	0.1942 +j0.4120	0.1942 +j0.4120	0.1942 +j0.4120	6108	5617	7372	6778	4.25	0.0055	0.0141	0.0365	0.0057	0.0057	0.0365	0.0057	0.0057	0.0365	0.0057	0.0057	0.0365
7	OH_XARM	336 ACSR	2684	2.23	0.1063 +j0.4397	0.2444 +j0.5562	0.2444 +j0.5562	0.2444 +j0.5562	5108	4637	6365	5452	3.80	0.0087	0.0449	0.0691	0.0081	0.0081	0.0691	0.0081	0.0081	0.0691	0.0081	0.0081	0.0691
8	OH_XARM	336 ACSR	2684	2.42	0.1063 +j0.4397	0.2444 +j0.5562	0.2444 +j0.5562	0.2444 +j0.5562	5108	4427	6360	5205	3.80	0.0087	0.0449	0.0691	0.0081	0.0081	0.0691	0.0081	0.0081	0.0691	0.0081	0.0081	0.0691
9	OH_XARM	336 ACSR	2096	2.81	0.1245 +j0.4493	0.3058 +j0.6395	0.3058 +j0.6395	0.3058 +j0.6395	4427	3906	5493	4539	3.61	0.0062	0.0379	0.0431	0.0095	0.0095	0.0379	0.0095	0.0095	0.0379	0.0095	0.0095	0.0379
10	OH_XARM	336 ACSR	2606	3.29	0.1438 +j0.4945	0.3572 +j0.6270	0.3572 +j0.6270	0.3572 +j0.6270	4279	3424	4919	3936	3.44	0.0062	0.0453	0.0515	0.0130	0.0130	0.0453	0.0130	0.0130	0.0453	0.0130	0.0130	0.0453
11	OH_XARM	336 ACSR	1377	7	0.1139 +j0.4246	0.3277 +j0.6244	0.3277 +j0.6244	0.3277 +j0.6244	5013	4231	5859	4953	3.73	0.0065	0.0249	0.0283	0.0720	0.0720	0.0249	0.0720	0.0720	0.0249	0.0720	0.0720	0.0249
12	OH_XARM	336 ACSR	1025	7	0.1344 +j0.4724	0.3321 +j0.6249	0.3321 +j0.6249	0.3321 +j0.6249	4487	3644	5184	4200	3.52	0.0311	0.0272	0.0327	0.0726	0.0726	0.0272	0.0726	0.0726	0.0272	0.0726	0.0726	0.0272
13	OH_XARM	336 ACSR	961	12	0.1517 +j0.4958	0.3809 +j0.6355	0.3809 +j0.6355	0.3809 +j0.6355	4226	3371	4759	3780	3.07	0.0273	0.0234	0.0469	0.0726	0.0726	0.0234	0.0726	0.0726	0.0234	0.0726	0.0726	0.0234
14	OH_XARM	336 ACSR	961	12	0.1517 +j0.4958	0.3809 +j0.6355	0.3809 +j0.6355	0.3809 +j0.6355	4226	3371	4759	3780	3.07	0.0273	0.0234	0.0469	0.0726	0.0726	0.0234	0.0726	0.0726	0.0234	0.0726	0.0726	0.0234
15	DE_28kV_XLPE	500	778	3.39	0.1479 +j0.4953	0.3670 +j0.6170	0.3670 +j0.6170	0.3670 +j0.6170	4263	3426	4872	3916	3.36	0.0061	0.0065	0.0152	0.0038	0.0038	0.0152	0.0038	0.0038	0.0152	0.0038	0.0038	0.0152
16	OH_XARM	336 ACSR	1659	3.65	0.1592 +j0.5217	0.3970 +j0.6923	0.3970 +j0.6923	0.3970 +j0.6923	4040	3196	4596	3636	3.28	0.0113	0.0264	0.0300	0.0753	0.0753	0.0264	0.0753	0.0753	0.0264	0.0753	0.0753	0.0264
17	OH_XARM	336 ACSR	1129	3.88	0.1679 +j0.5421	0.4201 +j0.6923	0.4201 +j0.6923	0.4201 +j0.6923	3863	2953	4403	3445	3.23	0.0087	0.0204	0.0232	0.0590	0.0590	0.0204	0.0590	0.0590	0.0204	0.0590	0.0590	0.0204
18	OH_XARM	336 ACSR	578	3.98	0.1724 +j0.5525	0.4320 +j0.6925	0.4320 +j0.6925	0.4320 +j0.6925	3687	2953	4310	3355	3.21	0.0045	0.0074	0.0119	0.0302	0.0302	0.0074	0.0302	0.0302	0.0074	0.0302	0.0302	0.0074
19	OH_XARM	336 ACSR	412	3.74	0.1624 +j0.5291	0.4054 +j0.6148	0.4054 +j0.6148	0.4054 +j0.6148	3981	3137	4523	3554	3.26	0.0032	0.0074	0.0095	0.0215	0.0215	0.0074	0.0215	0.0215	0.0074	0.0215	0.0215	0.0074
20	OH_XARM	336 ACSR	3650	4.47	0.1921 +j0.5387	0.4845 +j0.6880	0.4845 +j0.6880	0.4845 +j0.6880	3505	2622	3944	3007	3.12	0.0297	0.0695	0.0791	0.2014	0.2014	0.0695	0.2014	0.2014	0.0695	0.2014	0.2014	0.0695
21	OH_XARM	336 ACSR	4634	5.39	0.2294 +j0.6580	0.5638 +j0.6580	0.5638 +j0.6580	0.5638 +j0.6580	3046	2252	3389	2513	2.89	0.0373	0.0873	0.0993	0.2528	0.2528	0.0873	0.2528	0.2528	0.0873	0.2528	0.2528	0.0873
22	OH_XARM	336 ACSR	2735	4.98	0.2192 +j0.6481	0.5407 +j0.6582	0.5407 +j0.6582	0.5407 +j0.6582	3230	2417	3616	2706	3.04	0.0211	0.0494	0.0562	0.1430	0.1430	0.0494	0.1430	0.1430	0.0494	0.1430	0.1430	0.0494
23	OH_XARM	336 ACSR	2671	5.47	0.2331 +j0.6945	0.5935 +j0.6945	0.5935 +j0.6945	0.5935 +j0.6945	3008	2218	3353	2473	2.88	0.0189	0.0464	0.0528	0.1345	0.1345	0.0464	0.1345	0.1345	0.0464	0.1345	0.1345	0.0464

PREVIOUS PUBLICATIONS

1. Presented at WPRC 2004.
2. Presented at TAMU 2005.